JAPANESE JOURNAL OF APPLIED PHYSICS
VOL. 29, NO. 7, JULY, 1990, pp. 1372–1376

A Useful Method for the Determination of the Total Electron Scattering Cross Section

Hiroyuki NISHIMURA and Takeji SAKAE†

Department of Physics, Niigata University, 8050 Ikarashi, Niigata 950-21
†Department of Nuclear Engineering, Kyushuu University,
6-10-1 Hakozaki, Higashiku, Fukuoka 812

(Received March 15, 1990; accepted for publication May 19, 1990)

A compact linear electron transmission apparatus has been constructed for the measurement of the total electron-scattering cross section for various atoms and molecules. The transmitted electrons are analyzed without a retarding potential. The effective scattering path length of electrons in the apparatus can be evaluated from measured currents. As a test of this method, the total electron-scattering cross section for CH_4 has been measured in the energy range between 5 and 500 eV with a statistical uncertainty $\leq 5\%$ for electrons below 250 eV and $\leq 7\%$ for electrons above 250 eV. The results show $E^{-1/2}$ dependence at lower energies and a steeper decline at higher energies.

KEYWORDS: experimental apparatus, electron transmission, cross section, methane, experiment

§1. Introduction

The total cross section (hereafter abbreviated as TCS) for electron scattering with an atom or molecule can be determined without any normalization procedure. Therefore the TCS serves as a normalization standard for various scattering cross sections. Methods for the determination of the TCS can be grouped into three classes; the first is the Ramsauer-type method,[1,2] the second is the time-of-flight method (TOF),[3] and the third is the linear electron transmission method.[4] In the first method, incident and transmitted electrons are momentum-selected with a uniform magnetic field. In the second method, transmitted electrons are discriminated from the scattered ones by means of their time-resolved spectra, which are detected after they have traveled some fixed distance. In the third method, attenuation of electron beam intensity passed through a collision cell is measured by an electron collector with or without retarding potential. The first and the second methods are suitable for the measurement of the TCS with high energy resolution at lower electron energies. The third method is useful for the determination of the TCS over a wide energy range. This method is also useful for observing gross features in the TCS.

In almost all of the measurements with linear transmission apparatuses, a retarding potential was used, with only a few exceptions, to discriminate inelastically scattered electrons from transmitted electrons. Floeder *et al.*[5] discriminated inelastically forward-scattered electrons (with energy losses above 2 eV) by applying a retarding potential on the field lens. Sueoka and Mori[6] applied a retarding potential 1.5 eV lower than that on a retarding element in a study of e-CH_4 collisions. Kauppila *et al.*[7] adjusted the retarding potential so as to decrease the beam intensity by about 20% in comparison with the case of no retarding potential. The linear transmission method with retarding potential is effective for measurement with monoenergetic electrons. However, it is hard to separate electrons elastically scattered at small angles from inelastically scattered electrons with small amounts of energy losses after the rotational and the vibrational excitation of target molecules. A much higher retarding potential would prohibit the arrival of a part of the transmitted electrons at the Faraday cup, and then results would give too high TCS values. In contrast, a lower retarding potential may introduce a part of the inelastically scattered electrons into the transmitted beam, and then results will give too low TCS values.

Jost and Ohnemus.[4] discussed the character of their linear transmission apparatus in detail and concluded that the high angular resolution measurement is more essential for TCS study than the high energy resolution measurement. We take the same standpoint as Jost and Ohnemus did. Although we do not deny the necessity of the separation of inelastically scattered electrons at a forward narrow angle from the transmitted electrons, we emphasize the importance of the high angular resolution in the TCS measurement.

For obtaining reliable TCS values, careful consideration is needed in the following aspects: first, a precise evaluation of the current to the collision volume; second, the evaluation of the effective electron path length; third, the evaluation of the scattered electrons which are sent to the Faraday cup together with transmitted electrons. We have fully examined all of these points experimentally. In this report, an improved transmission technique with no retarding potential is presented. For convenience, the electron energy is chosen in the range between 5 and 500 eV.

The reliability of this method is tested in the e-CH_4 scattering. Many workers studied CH_4 as a prototype of polyatomic molecules, and because of the need of data in studies on planetary atmosphere and gaseous discharge. Therefore it is possible to compare the present result with those of measurements with various methods. Recent experimental results are those reported by Floeder *et al.*[5] (transmission, 5–400 eV), by Sueoka and Mori[6] (TOF with magnetic fields of 1–400 eV), by Ferch *et al.*[8] (TOF, 0.085–12 eV), by Jones[9] (TOF, 1.3–50 eV), by Lohmann

and Buckman[10] (TOF 0.1–20 eV), and by Dababneh *et al.*[11] (transmission with magnetic fields of 4.5–500 eV). Various theoretical calculations are reviewed by Jain[12] and by Yuan.[13] Despite those efforts, some discrepancies exist among the results at lower energies; especially, the recent results of ref. 6 are about 13% lower on the average than those of ref. 11 at energies below 200 eV. For the establishment of the TCS for e-CH_4, a more detailed measurement is clearly needed.

§2. Experimental

2.1 *Apparatus*

The apparatus used in this experiment is shown in Fig. 1. This is essentially the same as the apparatus used previously,[14] except for a drift cell (DC) set between a collision cell (CC) and a Faraday cup (FC) for the determination of the effective path length of the transmitted electrons. Electrons from a tungsten filament are accelerated by a Pierce-type electron gun toward aperture A_1 and are collimated by aperture slits A_1–A_6, whose opening diameters are 0.6, 1.0, 1.0, 1.0, 0.6 and 1.0 mm. An electron beam collimator was designed originally as an electrostatic cylindrical lens to prepare a monochromatic electron beam. However, for the simple operation of the apparatus over a wide energy range, all lens elements are grounded. Apertures A_7–A_9 (exit apertures) have the same opening diameter and define the angular spread of electrons viewed from the FC. In each run, the aperture size of 1.0, 1.4, 1.7, or 2.0 mm in diameter was used. Apertures A_6 and A_{10} have a slightly larger opening diameter than that of A_5 and A_9 so as to allow the transmission of unscattered electrons and to stop scattered electrons in each cell as much as possible. Aperture A_8 also has a function similar to that of A_6 and A_{10}. All apertures and inside cylinders of the DC and the FC are made of molybdenum.

The electron gun, beam collimator, CC, DC and FC are made of stainless steel (type 310) and are insulated independently with thin Teflon layers. Electron currents received at the CC, DC, and FC are measured with independent electrometers (ADVANTEST TR 8651). The side walls of the CC and DC are made of two concentric cylinders for the complete collection of scattered electrons. For the supply of the target gas from a reservoir to the CC and then to the manometer, shallow grooves are slotted on the outer surface of the inner cylinder of the CC. Some gas effuses from the CC to the DC and causes the effective path length of electrons to become longer than designed. It is therefore necessary to pump out the gas in DC as rapidly as possible. Each cylinder in the DC has a pair of holes (5 mm in diameter) facing each other across the axis. The assembly of the cylinder is shown schematically in Fig. 2. The purpose of this design is to allow the gas to effuse out efficiently and at the same time, to prevent electrons from being lost. In particular, there is an additional feature in the inner cylinder. The outer surface has a groove of width 8 mm and of depth 1 mm, i.e., sufficiently wide to cover the holes, which provides, together with the outer cylinder, a shallow pass to let the gas flow.

The temperature of the CC was monitored with a calibrated thermistor attached to the outer surface of the CC. The vacuum vessel (type 304L stainless steel, 15.5

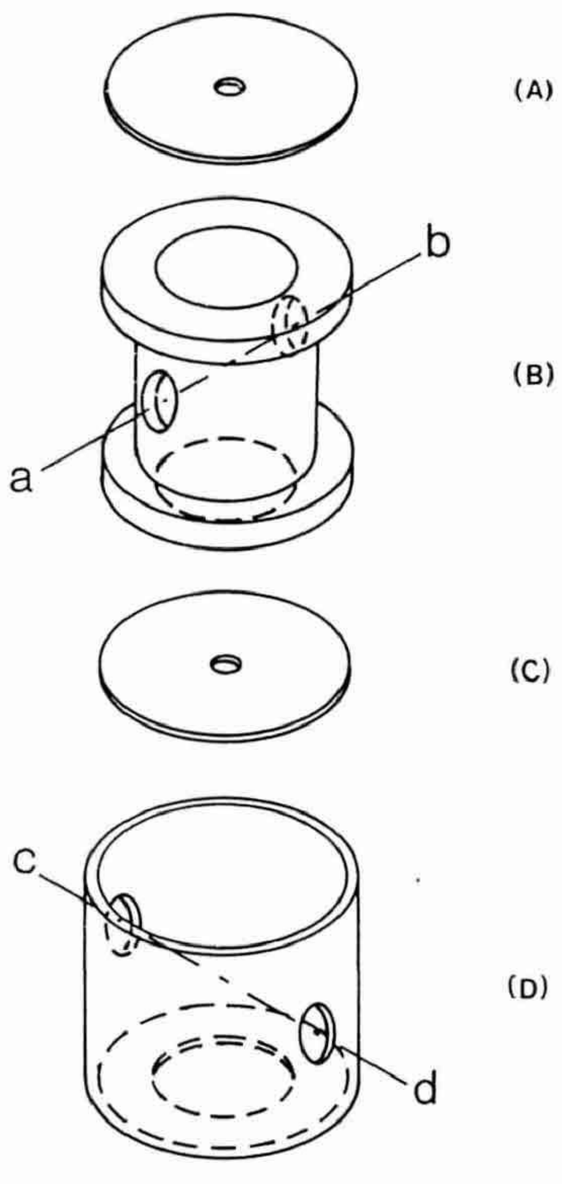

Fig. 2. Assembly of DC. Lateral axis ab of (B) crosses with cd of (D) at right angles. (A), Aperture A_6 (molybdenum). (B), Inner cylinder (molybdenum). (C), Aperture A_5 (molybdenum). (D), Outer cylinder (stainless steel, type 310).

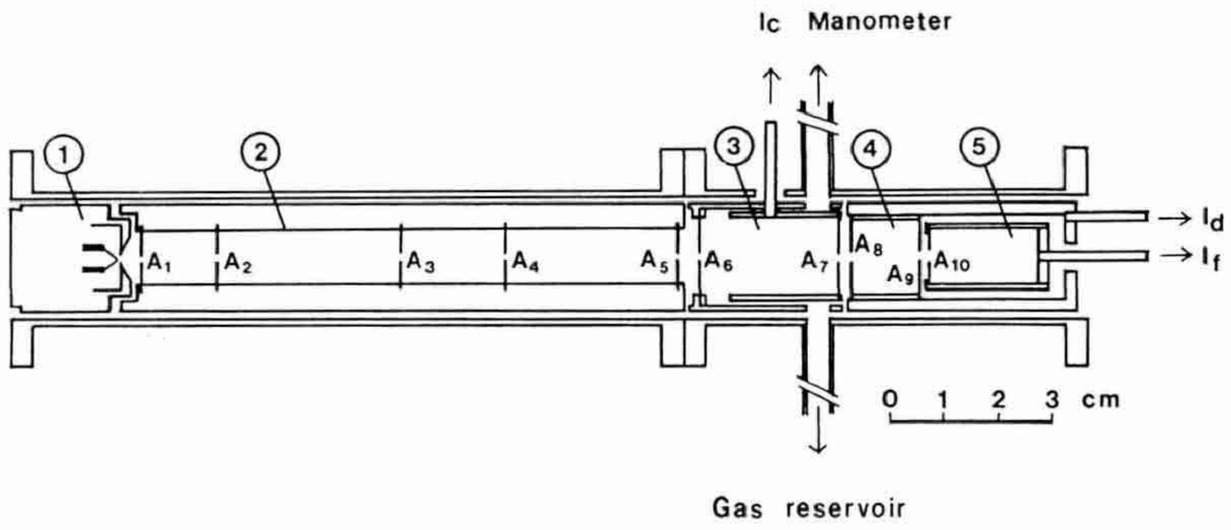

Fig. 1. Schematic diagram of the apparatus. 1, Electron gun; 2, Electron beam collimator; 3, Collision cell (CC); 4, Drift cell (DC); 5, Faraday cup (FC); A_1–A_{10}, Aperture slits.

cm in inner diameter and 50 cm in length) is evacuated by a 6-inch oil diffusion pump with a liquid nitrogen trap to the base pressure of about 3×10^{-7} Torr. During the measurement, the pressure in the vessel was kept below a few times 10^{-6} Torr.

The earth's magnetic field near the apparatus was kept below 3 mG with a concentric mu-metal cylinder placed inside the vessel. The purity of the target gas (CH_4) was 99.99% according to the supplier, and no further purification was performed.

2.2 *Procedure*

The total electron-scattering cross section $\sigma(E)$ is defined by

$$I_F=I_0\exp[-N\sigma(E)L], \tag{1}$$

where I_0 is the incident current, I_F is the transmitted current, N is the number density of the target molecule, and L is the effective collision path length. The current received at each section is read by the electrometers, varying the target gas pressure under the single electron-scattering condition. The pressure is adjusted in the range between I and 5 mTorr. The incident electron current was adjusted below 100 pA. Under those conditions, the measured TCS was independent of the target gas pressure and the incident current intensity. The incident total current I_{tot} is given by the sum of the measured currents, namely, I_C at the CC, I_D at the DC, and I_F at the FC, i.e.,

$$I_{tot}=I_C+I_D+I_F. \tag{2}$$

Owing to the geometry of the apparatus, a finite fraction η of the incident beam will arrive at the FC through the CC and DC when the electron beam suffers no scattering within the cell. The true incident current I_0 is given as

$$I_0=\eta(I_C+I_D+I_F). \tag{3}$$

As in the previous study,[14] each of the currents on the right-hand side of eq. (3) is measured at two target gas pressures. Substituting those values into eq. (1), we obtain the relation

$$\ln\frac{I_{F1}I_{tot2}}{I_{F2}I_{tot1}}=(N_2-N_1)\sigma L, \tag{4}$$

where the subscripts indicate two values of the target gas pressure.

Next, we discuss procedures for determining the electron path length and the transmitted electron current. The apparent electron path length L_a is given by

$$L_a=l_0+l_g+l_1(E), \tag{5}$$

where l_0 is the designed length of the CC, l_g is the gap distance between the CC and DC, or the distance between A_7 and A_8 in Fig. 1, and $l_1(E)$ is the apparent extended electron path length in the DC which is caused by the effusion of the target gas from the CC. The extended path length $l_1(E)$ is given as

$$l_1(E)=l_{10}-\Delta l(E). \tag{6}$$

The length l_{10} is a true extended electron path length in the DC. It may be given by gas kinematics, with consideration of the real geometrical structure of the CC, and of the other kinematical conditions of the gas in the CC and DC. The correction term $\Delta l(E)$ in eq. (6) accounts for the scattering of electrons in the CC. The true path length L_t is then

$$L_t=l_0+l_g+l_{10}. \tag{7}$$

If we can neglect l_{10} and l_g in comparison with l_0, eq. (1) is written as

$$I_F=I_0\exp[-N\sigma_0(E)l_0]. \tag{8}$$

If we cannot neglect l_{10} and l_g in comparison with l_0, we need careful evaluation of the electron path length. Then eq. (1) is rewritten using eq. (5) and eq. (6) as

$$\begin{aligned} I_F&=I_0\exp[-N\sigma_d(E)L_a],\\ &=I_0\exp\{-N\sigma_d(E)[l_0+l_g+l_1(E)]\}, &(9)\\ &=I_0\exp\{-N\sigma_d(E)[l_0+l_g+l_{10}-\Delta l(E)]\}, &(10)\end{aligned}$$

where σ_d is a measured TCS value with an opening diameter d of the exit aperture. The term $\exp[N\sigma_d\Delta l(E)]$ in eq. (10) represents an excess component included in the transmitted current I_F. Therefore L_a gives the effective path length.

In the first step, $\sigma_0(E)$ in eq. (8) is determined using N, l_0, I_0, and I_F. In the next step, $l_1(E)$ is determined by combining the above $\sigma_0(E)$ with I_D and I_F. Replacing l_0 in eq. (8) by $L_a=l_0+l_g+l_1(E)$, one determines σ_d from eq. (9). The true extended electron path length l_{10} in DC can be evaluated, if it is needed, from the behavior of $l_1(E)$ at high energies. Typical behavior of $l_1(E)$ is illustrated in Fig. 3.

Through the evaluation of the electron path length, the gap between A_5 and A_6 (1 mm in length) is not considered explicitly, The gap is directly opened to the vacuum vessel so as to evacuate efficiently the gas effused from the CC to the vacuum vessel through A_6 (1.0 mm in diameter). The ratio of the opening area of A_5 (0.6 mm in diameter) to that of A_6 is about 1/3. Therefore only a small amount of target gas will stream into the electron collimator through A_5. Taking into consideration the gap length, the uncertainty of the true path length is 3% or less.

The correction procedure discussed above is not sufficient for obtaining the true TCS (σ_t) because electrons scattered in the CC and DC into a narrow forward angle can arrive at the FC through apertures A_7–A_9. The TCS σ_t should be determined as the measured σ_d with infinitesimal diameter of apertures A_7–A_9. Actually, meas-

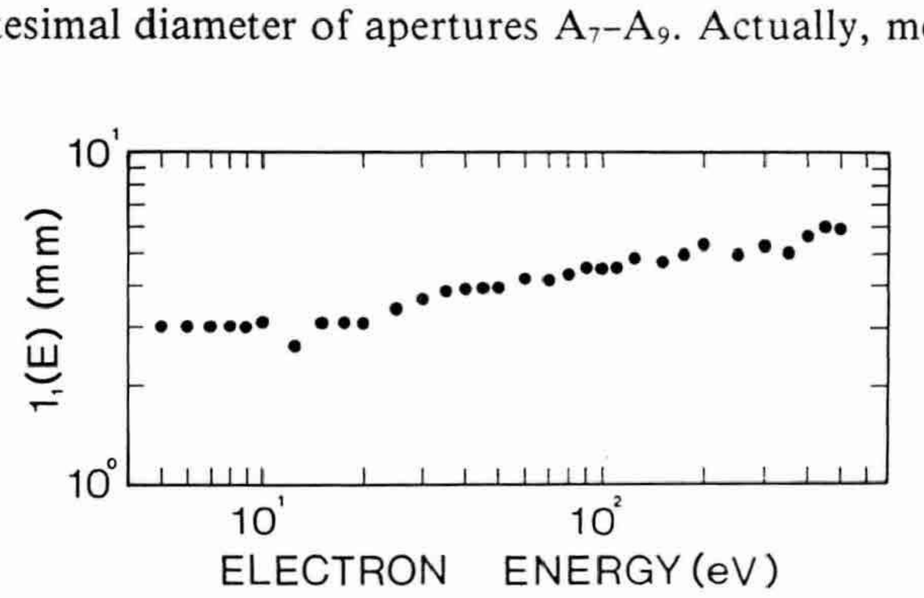

Fig. 3. Effective path length $l_1(E)$ extended into DC vs electron energy.

urements of σ_d are repeated with d set at 1.0, 1.4, 1.7, and 2.0 mm. The TCS σ_t is determined by extrapolating the measured σ_d at $d=0$. We assume a simple relation between σ_t and σ_d,

$$\sigma_d=\sigma_t-\pi(d/2)^2\delta\sigma, \tag{11}$$

where $\delta\sigma$ is a correction factor for σ_d.

In the above procedure, one may feel some misgivings about the treatment of inelastically scattered electrons included in I_F. However, the intensity of inelastically scattered electrons from molecules has a finite value at each scattering angle. Therefore, we can make the effect of those electrons for the determination of TCS negligibly small in this manner.

The thermal transpiration effect is also considered for the correction of the target gas pressure because the temperature around the CC was in the range between 20°C and 35°C, whereas the manometer was kept at 45°C during the measurement.

The electron-energy scale is calibrated by observing the 19.36-eV resonance in He. For this aim, helium is introduced into the CC. Recorder traces of the current received at the CC and FC are shown in Fig. 4. The profile of the resonance appeared at a nominal energy of 18.4 eV. The difference of the above two values 0.9 eV gives the instrumental displacement from the true electron energy. The profile of the resonance tells us that the energy width (full width at half-maximum (FWHM)) of the incident beam is about 0.5 eV at around 19.36 eV.

The total systematic uncertainty is estimated from the quadratic sum of the individual uncertainties. The major part of the systematic uncertainty come out of two experimental procedures: one is the evaluation of the total current defined by eq. (2) and the other is the determination of σ_t from σ_d using eq. (11). The resultant systematic uncertainty is 13%. The sources of the uncertainties are listed in Table I.

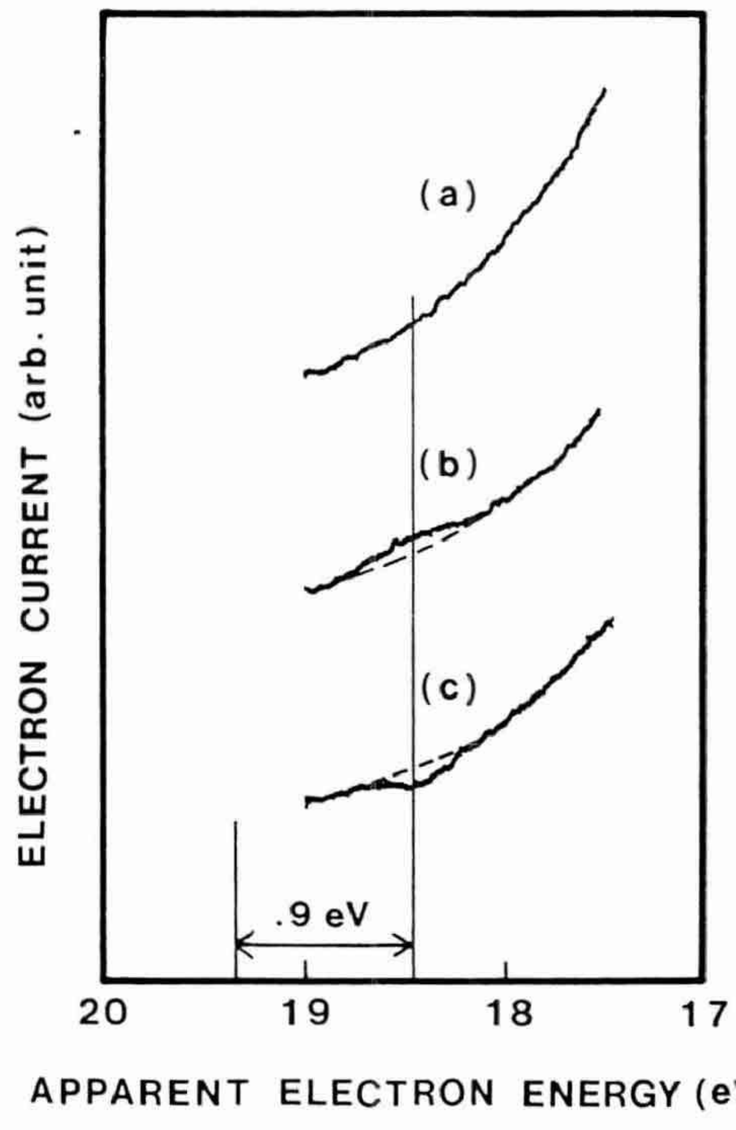

Fig. 4. Scattered electron intensity from He vs electron energy: (a), Received at Faraday cup with no He in CC; (b), Received at Faraday cup with He (5 mTorr) in CC; (C), Received at CC with He (5 mTorr).

Table I. Systematic uncertainty (%).

Pressure	Current	Scattering length	σ_d	σ_t
0.6	5 for I_F 5 for I_C 5 for I_D	3	9	13

§3. Results and Discussion

Table II lists TCS values as well as their statistical uncertainties. The final TCS values σ_t are determined from analysis of measured σ_d with different d's. Relatively large values of the statistical error in the TCS at high energies result from this procedure. Below 40 eV, results are independent of d, the diameter of the exit opening. Above 40 eV, however, there is slight dependence of σ_d TCS on d, which becomes progressively stronger at higher energies. The data of Table II show a maximum at around 8 eV. A small shoulder at around 50–100 eV may be attributed to inelastic processes including ionization and dissociation.

Vogt and Wannier[15] gave a simple expression for the scattering cross section of a charged particle (including electron) from the polarization potential of a molecule:

$$\sigma=\text{const}\cdot(e^2\alpha/mv^2)^{1/2}, \tag{12}$$

where e is the electron charge, α is the molecular polarizability, m is the reduced mass and v is the relative velocity between colliding particles. Bromberg[16] also showed that the polarization potential dominates the elastic scattering into a small forward angle and gave a similar result. For convenience, eq. (12) is rewritten simply as

$$\sigma\,(\text{Å}^2)=aE^{-1/2}. \tag{13}$$

Figure 5 shows experimentally determined TCS values as a function of electron energy with a fitted line. Four

Table II. Total electron-scattering cross section for CH_4. The numbers in parentheses indicate statistical errors.

Energy (eV)	σ_t (Å^2)	Energy (eV)	σ_t (Å^2)
5	20.92 (0.39)	60	11.88 (0.35)
6	23.83 (0.31)	70	10.73 (0.25)
7	26.47 (0.24)	80	10.25 (0.33)
8	26.46 (0.84)	90	9.48 (0.20)
9	27.07 (1.16)	100	9.01 (0.23)
10	25.65 (0.33)	110	8.59 (0.12)
12.5	24.20 (0.64)	125	7.92 (0.21)
15	22.42 (0.50)	150	7.05 (0.29)
17.5	21.00 (0.26)	175	6.42 (0.23)
20	19.38 (0.42)	200	5.84 (0.19)
25	17.43 (0.43)	250	4.98 (0.36)
30	15.90 (0.31)	300	4.31 (0.16)
35	14.75 (0.15)	350	3.76 (0.17)
40	13.81 (0.27)	400	3.37 (0.20)
45	13.41 (0.39)	450	3.02 (0.13)
50	13.03 (0.61)	500	2.75 (0.11)

broken curves labeled A, B, C, and D are the measured σ_d taken by changing the diameter of the aperture set (A_7–A_9). Between 12.5 and 175 eV, a fit within 3% is achieved with $a=87.84\pm1.70$ Å^2 eV.$^{1/2}$ (As an exception, at 50, 60 and 80 eV, there are somewhat larger deviations.) Above 400 eV, σ_t decreases with increasing energy more rapidly than $E.^{-1/2}$

In Table III, values of the coefficient a in eq. (13) are listed, which are obtained by fitting each result to eq. (13). Each value is an average over the cited energy range and their standard deviation. A similar empirical formula with a correction term has been presented by Floeder *et al.*[5] They fitted their data at energies between 100 and 400 eV with a value lower than that listed above. The present results, as well as those of Jones and of Dababneh *et al.*, can all be fitted to eq. (13) with a slight deviation. The results of Floeder *et al.* and those of Sueoka and Mori can be fitted to a line with a slightly more gentle decline than $E^{-1/2}$ in the overlapped energy range.

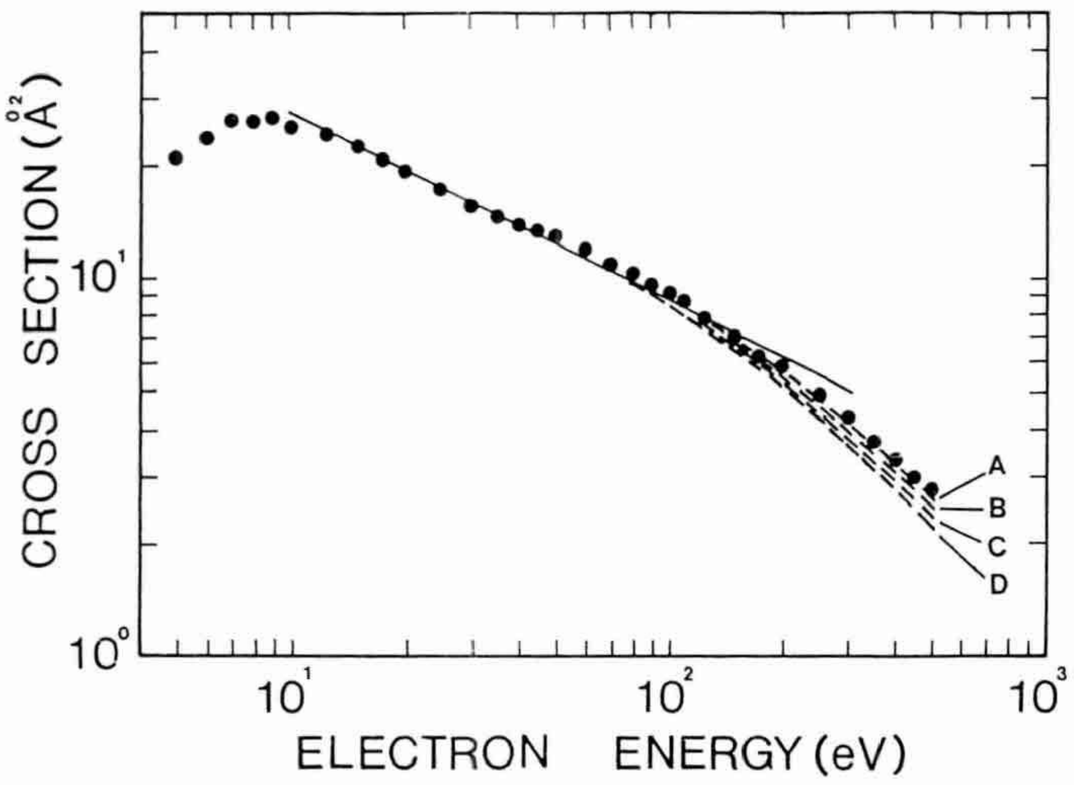

Fig. 5. The measured cross section vs electron energy and its asymptotic line. The line represents σ (Å^2)$=87.84E.^{-1/2}$ Broken curves A, B, C, and D indicate σ_d with $d=1.0$, 1.4, 1.7, and 2.0 mm, respectively.

Table III. Coefficient a in eq. 13

Author	a (Å^2 eV$^{1/2}$)	Energy range (eV)
Present authors	87.84±1.70	12.5−175
Floeder *et al.* (ref. 5)	82.81±6.15	12.5−200
Jones (ref. 9)	85.85±1.02	12.5−50
Sueoka and Mori	78.93±3.59	12.5−200
Dababneh *et al.* (ref. 11)	89.75±1.75	12.5−200

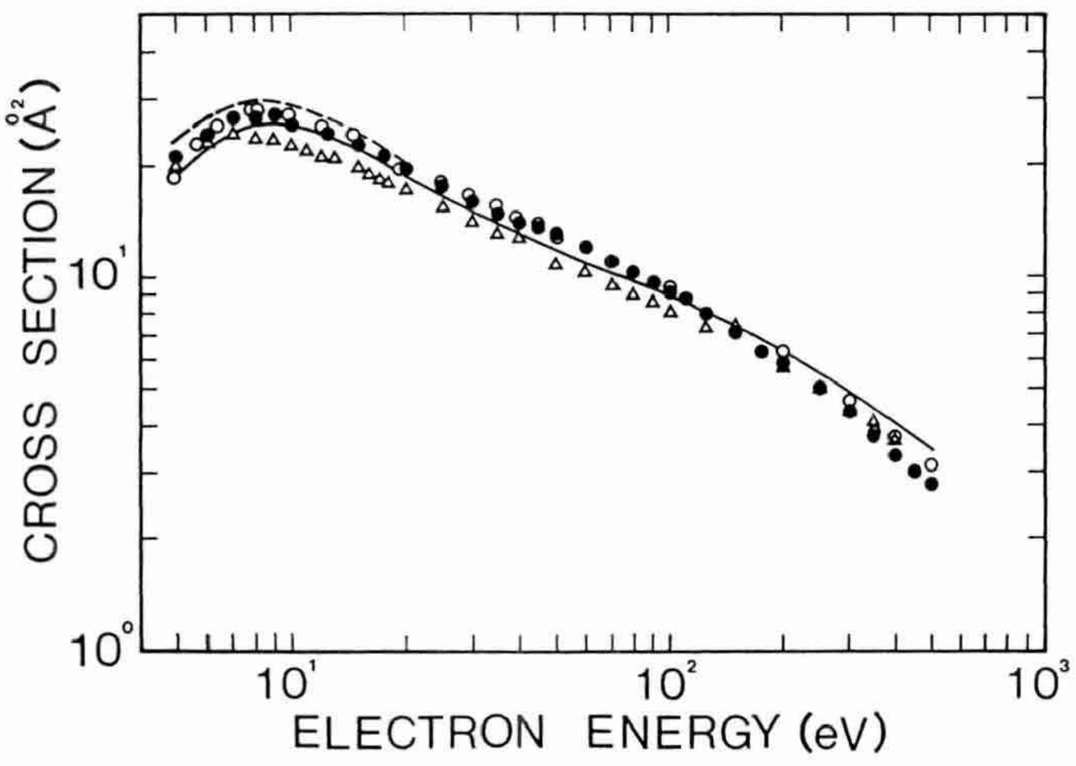

Fig. 6. Comparison of the present result with those of the recent experiments and theoretical calculations: ●, Present result; △, Sueoka and Mori (ref.6); ○, Dababneh *et al.* (ref. 11); ——, Jain (ref. 12); – – – –, Yuan (ref. 13).

Figure 6 shows a comparison with recent experimental and theoretical results. The agreement between the present result and that of Jones[9] is excellent. (To avoid confusion, Jones's result is not shown in the figure). The result of Dababneh *et al.*[11] is slightly higher than the present result. The result of Sueoka and Mori[6] is lower by about 10–13% below 100 eV, and somewhat higher at higher energies than the present result. Other recent experimental results[5,8-10] distribute between those of Dababneh *et al.* and of Sueoka and Mori. Various principles for the discrimination of the scattered electrons may explain the discrepancies among the measured TCS values.

The calculation of Giantarco and Scialla[17] by the modified empirical exchange approximation agrees very well with the present result in the energy range where the results can be compared. The calculation of Jain[12] with the spherical approximation (SEAPTJa) also agrees very well with the present result in the energy range below 200 eV. The theoretical result of Yuan[13] with the modified exact static exchange approximation is slightly higher than the present result.

Acknowledgments

Authors would like to express their gratitude to Dr. M. Inokuti for his critical reading of earlier manuscripts. One of the authors (H. N.) thanks Dr. S. Trajimar and Professor H. Tawara for their continuous interest in this work and also thanks K. Sasazawa for her valuable assistance.

References

1) C. Ramsauer: Ann. Phys. **66** (1921) 546.
2) D. E. Golden and H. W. Bandle: Phys. Rev. **138** (1965) A14.
3) R. E. Kennerly: Rev. Sci. Instrum. **48** (1977) 1682.
4) K. Jost and B. Ohnemus: Phys. Rev. A **19** (1979) 641.
5) K. Floeder, D. Fromme, W. Raith, A. Schwab and G. Sinapius: J. Phys. B **18** (1985) 3347.
6) O. Sueoka and S. Mori: J. Phys. B **19** (1986) 4035.
7) W. E. Kauppila, T. S. Stein, G. Jesion, M. S. Dababneh and V. Pol: Rev. Sci. Instrum. **48** (1977) 822.
8) J. Ferch, B. Granitza and W. Raith: J. Phys. B **18** (1985) L450.
9) R. K. Jones: J. Chem. Phys. **82** (1985) 5424.
10) B. Lohmann and S. J. Buckman: J. Phys. B **19** (1986) 2565.
11) M. S. Dababneh, Y.-F. Hsieh, W. E. Kauppila, C. K. Kwan, Steven J. Smith, T. S. Stein and M. U. Uddin: Phys. Rev. A **38** (1988) 1207.
12) A. Jain: Phys. Rev. A **34** (1986) 3707.
13) J. Yuan: J. Phys. B **21** (1988) 3113.
14) H. Nishimura and K. Yano: J. Phys. Soc. Jpn. **57** (1988) 1951.
15) E. Vogt and G. H. Wannier: Phys. Rev. **95** (1954) 1190.
16) J. P. Bromberg: J. Chem. Phys. **51** (1969) 4117.
17) F. A. Giantarco and S. Scialla: J. Phys. B **20** (1978) 3171.